Immune regulators SIB1 and LSD1 antagonistically regulate PhANGs via the GLK transcription factors

Mengping Li[1,2,a], Keun Pyo Lee[1,a], Tong Liu[1,2], Vivek Dogra[1,3], Jianli Duan[1], Mengshuang Li[1,2], Weiman Xing[1], and Chanhong Kim[1,b]

[1] Shanghai Center for Plant Stress Biology and CAS Center for Excellence in Molecular Plant Sciences, Chinese Academy of Sciences, Shanghai 200032, China.

[2] University of the Chinese Academy of Sciences, Beijing 100049, China.

[3] Present address: Biotechnology Division, CSIR-Institute of Himalayan Bioresource Technology, Palampur 176061, India

[a] These authors contributed equally to this work.

[b] Address correspondence to chanhongkim@sibs.ac.cn

Abstract

GOLDEN2-LIKE (GLK) transcription factors drive the expression of photosynthesis-associated nuclear genes (PhANGs), indispensable for chloroplast biogenesis. We previously demonstrated that the salicylic acid (SA)-induced SIGMA FACTOR-BINDING PROTEIN1 (SIB1), a transcription coregulator and positive regulator of SA-primed cell death, interacts with GLKs. The SIB1-GLK interaction raises the level of light-harvesting antenna proteins in the photosystem II, aggravating photoinhibition and singlet oxygen ($^1O_2$) burst. $^1O_2$ then contributes to SA-primed cell death via EXECUTER1 (EX1, $^1O_2$ sensor protein)-mediated retrograde signaling upon reaching a critical level. We now reveal that LESION-SIMULATING DISEASE 1 (LSD1), a transcription coregulator and negative regulator of SA-primed cell death, interacts with GLKs to repress their activities. Consistently, the overexpression of LSD1 represses the expression of PhANGs, but the loss of LSD1 increases their expression. The SA-induced SIB1 then counteractively interacts with GLKs, leading to EX1-mediated cell death. Collectively, we provide a working model that mutually exclusive SA-signaling components SIB1 and LSD1 antagonistically regulate GLKs to fine-tune the expression of PhANGs, priming SA-induced cell death, and sustaining $^1O_2$ homeostasis, respectively.

Chloroplasts communicate with the nucleus via retrograde signaling (RS) to sustain photosynthetic homeostasis in response to the ever-changing environment. Upon exposure to unfavorable environmental conditions, chloroplasts downregulate photosynthesis-associated nuclear genes (PhANGs), referred to as biogenic RS, but stimulate the expression of stress-related genes via alternate RS pathways, collectively called operational RS. The nuclear-encoded chloroplast GENOMES UNCOUPLED 1 (GUN1) protein plays a pivotal role in the biogenic RS[1]. GUN1 integrates various retrograde signals released by the disturbance in plastid gene expression, reactive oxygen species (ROS) or redox homeostasis, and tetrapyrrole biosynthesis (TBS) in chloroplasts[1,2]. The well-known downstream targets of GUN1-mediated RS are two nuclear genes encoding the GOLDEN2-LIKE (GLK) transcription factors (TFs)[3,4]. In fact, GUN1-mediated RS represses *GLK* transcription. In *Arabidopsis thaliana* (Arabidopsis), GLK1 and GLK2 function redundantly to express PhANGs, promoting chloroplast biogenesis. Consistently, the loss of GLKs significantly impairs chloroplast biogenesis[5].

Recent studies discovered an unexpected function of GLKs towards plant immune responses. The steady-state levels of SA-responsive genes (SARGs) are significantly lower in GLK1-overexpressing (oxGLK1) Arabidopsis transgenic plants relative to wild-type (WT) plants[6]. Accordingly, the oxGLK1 plants are susceptible to the biotrophic pathogen *Hyaloperonospora arabidopsidis* (*Hpa*) Noco2, while *glk1 glk2* double knockout mutant plants are more resistant compared to WT plants[7]. However, other studies reported that the GLKs confer resistance towards the cereal fungal pathogen *Fusarium graminearum*[6], necrotrophic fungal pathogen *Botrytis cinerea*[7], and the Cucumber mosaic virus[8]. These findings indicate that there seem to be multiple regulatory circuits (positive and negative) toward GLK function to different microbial pathogens. Perhaps, various transcriptional coregulators distinctively induced (or activated) by pathogens may differently contribute to the GLK-mediated immune/stress responses.

We lately demonstrated that the nuclear-targeted SIGMA FACTOR-BINDING

PROTEIN 1 (SIB1), a defense-related transcription coregulator, interacts with GLKs in response to an increase in foliar salicylic acid (SA)[9]. In Arabidopsis *lesion-simulating disease 1* (*lsd1*), the increased level of SA rapidly induces the otherwise undetectable SIB1, facilitating its accumulation in both the nucleus and the chloroplasts[9,10]. The dual targeting of SIB1 was also observed in WT plants after SA treatment. The SIB1-GLK interaction in the nucleus enhanced the expression of PhANGs, while the chloroplast-localized SIB1 (cpSIB1) represses the expression of photosynthesis-associated plastid genes (PhAPGs)[9]. This concurrent uncoupled regulation of PhANGs and PhAPGs increases the levels of singlet oxygen ($^1O_2$) in chloroplasts, likely through enhanced photoinhibition in PSII[9]. EXECUTER1 (EX1), a $^1O_2$ sensor protein[11], then mediates $^1O_2$-triggered RS to induce cell death in *lsd1* mutant plants[9]. We also demonstrated that the nuclear form of SIB1 (nuSIB1) undergoes co-translational N-terminal acetylation (NTA) and post-translational ubiquitination. While the former case renders nuSIB1 more stable, the latter modification promotes its degradation via the ubiquitin-proteasome system (UPS) within a short period[12]. The NTA and UPS seem to finely regulate nuSIB1-mediated stress responses. Nonetheless, earlier reports regarding the positive role of both nuSIB1 and cpSIB1 to SA-primed cell death in *lsd1* mutant suggest that LSD1 may be required to repress the expression of PhANGs to sustain $^1O_2$ homeostasis.

Here, we demonstrate that LSD1, a transcription coregulator and negative regulator of SA-primed cell death, interacts with GLKs in the nucleus. LSD1 considerably reduces the GLK binding activity to the promoters of the examined PhANGs in Arabidopsis. In agreement, LSD1-overexpressing plants exhibit significantly reduced levels of PhANGs, while the loss of LSD1 causes a notable upregulation of PhANGs relative to WT plants. Most likely, SA intervenes the LSD1-GLK interaction through a rapid accumulation of nuSIB1, leading to an nuSIB1-GLKs interaction. We thus conclude that the defense-associated but mutually exclusive transcription coregulators nuSIB1 (positive regulator) and LSD1 (negative regulator) antagonistically regulate the expression of PhANGs through GLKs. Such a regulatory circuit may play an essential role in sustaining $^1O_2$ and photosynthetic

homeostasis under certain stress conditions wherein SA signaling primes plant stress responses.

Results

LSD1 interacts with the GOLDEN2-LIKE transcription factors GLK1 and GLK2

The stress hormone SA primes cell death in the *lsd1* mutant in a light-dependent manner, a typical characteristic of most lesion mimic mutants (LMMs)[9,13]. Upon exposure to various stimuli, including light, cold, UV-C, red light, hypoxia, and pathogens[13-20], *lsd1* mutant plants exhibit an uncontrolled foliar cell death, called runaway cell death (RCD). The SA-induced transcription coregulator nuSIB1 potentiates the expression of PhANGs and immune-related genes by modulating the TF activity of GLKs and WRKY33, respectively. Both GLK-nuSIB1 and WRKY33-nuSIB1 interactions contribute to *lsd1* RCD[9,10]. Alternatively, this finding suggests a possible antagonism between LSD1 and nuSIB1 because nuSIB1-driven immune responses occur in the absence of LSD1.

To reveal the LSD1 interactome, a potential target of nuSIB1, we generated Arabidopsis WT transgenic plants overexpressing GREEN FLUORESCENT PROTEIN (GFP)-tagged LSD1 under the control of the CaMV 35S promoter (35S). The immunoblot assay detected the LSD1-GFP fusion protein at the predicted molecular mass of approximately 46 kD using an anti-GFP antibody (Supplementary Fig. 1). Next, using magnetic beads conjugated with GFP antibody, we co-immunoprecipitated LSD1-GFP and its putative associated proteins. The trypsin-digested protein samples were then subjected to tandem mass spectrometry (MS) analyses. The two independent experiments of co-immunoprecipitation (Co-IP) coupled to MS analysis using two separately prepared biological samples identified 55 putative LSD1-associated proteins, which are absent in the protein samples of GFP-overexpressing transgenic plants (*35S*:*GFP*) (Supplementary Table 1).

Among the 55 proteins, we identified GLK1. In Arabidopsis, GLK1 and its

homolog GLK2 share around 50% amino acid sequence identity. Both contain two conserved domains, the DNA-binding domain (DBD) and the C-terminal GCT-box that is explicit in GLK TFs (Fig. 3a)[5,21]. A comparison of the DBD domain and the GCT-box between GLK1 and GLK2 shows a 90% and 79% identity, respectively[22]. Therefore, not only GLK1 but also GLK2 may interact with LSD1. To this end, we performed a bimolecular fluorescence complementation (BiFC) assay in *Nicotiana benthamiana* (*N. benthamiana*) leaves. Consistent with the previous report[15], we confirmed the LSD1-LSD1 interaction in the nucleus, as evident in the overlapped signals detected from the YELLOW FLUORESCENT PROTEIN (YFP) and the blue-fluorescent DNA stain 4', 6-diamidino-2-phenylindole (DAPI) (Fig. 1a). Similarly, we observed an equivalent yellow fluorescence signal of YFP in *N. benthamiana* leaf epidermal cells coexpressing LSD1-YFP^N and GLK1 (or GLK2)-YFP^C (Fig. 1a). All YFP signals were exclusively observed in the nucleus (Fig. 1a). The Co-IP and an ensuing immunoblot assay further corroborated the LSD1-GLK interaction (Fig. 1b). We also purified the full-length recombinant proteins of LSD1, GLK1, and GLK2 expressed in *Escherichia coli*. The following gel filtration assays demonstrated that either GLK1 (Fig. 2a) or GLK2 (Fig. 2b) form a complex with LSD1, as shown by their co-migration.

GLK interacts with LSD1 via the conserved region of the C-terminus

In GLKs (Fig. 3a), the C-terminal GCT-boxes drive the homo- or hetero-dimerization in maize[21]. In Arabidopsis, the *turnip yellow mosaic virus* (TYMV) protein P69 interacts with GLK1 and GLK2 proteins through the GCT-box to hinder their activities, leading to the repression of PhANGs and an impaired chloroplast biogenesis[23]. To define the necessary GLK region for its interaction with LSD1, we attempted to produce truncated GLK1 and GLK2 recombinant proteins. However, unlike GLK2 protein, we could not produce sufficient quantities of the truncated GLK1 variants retaining only the C-terminal conserved regions. Hence, as indicated in Fig. 3a, we used the recombinant proteins of the truncated GLK2 variants for the *in vitro* gel filtration assays. The results showed that the C-terminus containing the small

conserved region (Fig. 3a) is sufficient to interact with LSD1 (Fig. 3b). To validate this result *in vivo*, we generated various BiFC constructs using both GLK1 and GLK2. GFP-fused GLK1 and GLK2 proteins, intact versus the C-terminus-deleted (including the small conserved region) GLKs ($GLK1_{\Delta CT}$ and $GLK2_{\Delta CT}$), were transiently expressed in *N. benthamiana* leaves for their subcellular localization. The confocal images clearly showed no impact of the C-terminus deletion towards a nuclear-localization (Fig. 4a). The subsequent BiFC (Fig. 4b) and Co-IP (Fig. 4c) analyses verified the *in vitro* results indicating that the C-terminal part, including the small conserved region, is essential for the interaction with LSD1.

Loss of LSD1 upregulates GLK target genes

What could be the biological consequence of the LSD1-GLK interaction? Given that GLKs promote the expression of PhANGs[3], it is plausible that the loss of LSD1 may primarily affect the expression of GLK target genes. Presumably, it may also participate in the *lsd1* RCD. To find the affected genes either by the loss of LSD1 or of GLK1/GLK2, we compared the RNA sequencing (RNA-seq) data of *lsd1* (*lsd1* versus WT)[9] and *glk1 glk2* (*glk1 glk2* versus WT)[23]. As shown in Fig. 5a, one group of 91 genes (listed in Supplementary Data 1) are shared between the upregulated genes (395, at least twofold) in *lsd1* (Supplementary Data 2) and the downregulated genes (936, at least twofold) in *glk1 glk2* (Supplementary Data 3). When analyzing these 91 genes, looking at the biological processes, photosynthesis and light-harvesting in PSII are over-represented (*P*-value=1.42E-07) (Fig. 5b, Supplementary Data 4). The potentiated expression of PhANGs in *lsd1* versus WT plants is indicative of a negative role of LSD1 in GLK activity. To this end, we also examined the relative transcript abundance of PhANGs in LSD1-overexpressing Arabidopsis transgenic plants (hereafter *oxLSD1*) using reverse transcription quantitative PCR (RT-qPCR). The results indicated that the examined genes encoding light-harvesting chlorophyll *a*/*b* binding proteins (LHCBs in PSII and LHCA1 in PSI) were substantially repressed in *oxLSD1* relative to WT plants (Fig. 5c). *oxLSD1* plants exhibited comparable levels of *GLK1* and *GLK2* transcripts relative to WT (Supplementary Fig. 2), implying that the

reduced expression of PhANGs likely results from a post-translational regulation of GLKs.

LSD1 inhibits the DNA-binding activity of GLKs

Given that nuclear-localized LSD1 acts as a transcription coregulator and that LSD1 interacts with GLKs, it is conceivable that LSD1 might directly regulate the GLK DNA-binding activity. To explore this assumption, we performed a chromatin immunoprecipitation (ChIP) coupled with a qPCR analysis. The relative activity of GLK1 towards its target promoters was examined in the presence or absence of LSD1 using protoplasts isolated from the rosette leaves of *lsd1 glk1 glk2* triple mutant plants. It should be noted that both LSD1 and GLK1 are unstable, and even in 35S promoter-driven *GLK1* stable transgenic lines it is challenging to detect the protein[24,25]. Thus, we used the protoplast transient expression system to ensure a sufficient protein expression of both LSD1 and GLK1 to elucidate the impact of LSD1 on GLK1 function. The *35S:GLK1-4xMyc* was transiently coexpressed with either *35S:RED FLUORESCENT PROTEIN* (*RFP*) or *35S:LSD1-RFP* in the protoplasts. ChIP assays were then conveyed with the nuclear lysis from the transfected protoplasts. The agarose beads conjugated with anti-Myc antibody were used to pull down the Myc-tagged protein-DNA complex. The immunoprecipitated DNA was then analyzed using qPCR to compare the DNA-binding activity of GLK1 in the presence or absence of LSD1. Finally, we examined the relative expression of well-established GLK target genes such as *LHCB1.4*, *LHCB3*, and *LHCB6*[3]. The results demonstrated that the presence of LSD1 markedly reduced the DNA-binding activity of GLK1 to the promoters of the *LHCBs* genes (Fig. 5d).

LSD1-GLK interaction regulates chlorophyll biosynthesis in WT

We next validated the above ChIP assay result *in planta*. Considering the positive regulation of chlorophyll synthesis by GLK1[3] and the repression of GLK activity by LSD1 (Fig. 5a-d), it is tempting to hypothesize that loss of LSD1 might increases the rate of chlorophyll biosynthesis. By revisiting the previously published RNA-seq

data[9], we noticed that a set of chlorophyll synthesis genes including *glutamyl tRNA reductase* (*HEMA1*/*Glu-TR*), *genome uncoupled 4* (*GUN4*), *magnesium chelatase H subunit* (*GUN5*/*CHLH*), *magnesium protoporphyrin IX monomethyl ester cyclase* (*CHL27*/*CRD1*), *protochlorophyllide oxidoreductase A* (*PORA)*, and *chlorophyllide a oxygenase* (*CAO*) were markedly upregulated in *lsd1* before the onset of RCD (Fig. 6a,b). We then analyzed the aminolevulinic acid (δ-ALA, the common precursor of all tetrapyrroles) synthesis rate in light-grown *lsd1* mutant plants treated with levulinic acid (LA)[26], a competitive chemical inhibitor of δ-ALA dehydratase that catalyzes the synthesis of porphobilinogen through the asymmetric condensation of two δ-ALA molecules. It is important to note that the δ-ALA synthesis rate is also referred to as the relative chlorophyll synthesis rate[27,28] (Fig. 6a). In view of that FLUORESCENT (FLU) protein directly represses Glu-TR activity to inhibit protochlorophyllide (Pchlide) accumulation in the dark[29] (Fig. 6a) and that *flu* mutant plants exhibit a higher δ-ALA synthesis rate in the presence of LA[29], we used the *flu* mutant as a positive control.

Interestingly, the δ-ALA levels were almost comparable in *lsd1* and *flu* seedlings. The concurrent inactivation of both *FLU* and *LSD1* further increased the δ-ALA level (Fig. 6c). Since the Pchlide levels in the dark would indirectly reflect the rate of chlorophyll biosynthesis due to the absence of the enzyme(s) that catalyzes Pchlide turnover[30], we measured the Pchlide levels in dark-incubated plants of WT, *flu*, *lsd1*, and *lsd1 flu* using high-performance liquid chromatography analysis. Pchlide was highly upregulated in the plants lacking FLU in the dark, as demonstrate earlier[31] (Fig. 6d). It was remarkable that the loss of LSD1 raises the level of Pchlide (approximately 1.5-fold increase) in both WT and *flu* mutant backgrounds, corresponding with the positive effect of the *lsd1* mutation on the δ-ALA synthesis. However, the total chlorophyll levels between these genotypes were almost comparable (Supplementary Fig. 3). Considering that chlorophyll synthesis and catabolism pathways synchronously coordinate chlorophyll homeostasis[32], an excess amount of chlorophyll may immediately undergo degradation. Collectively, these

results corroborate the negative role of LSD1 towards GLK activity, which seems to be, at least in part, required for tetrapyrrole homeostasis.

SA-induced SIB1 intervenes LSD1-GLK1 interaction

Since SIB1-mediated genomes uncoupled expression of PhANGs and PhAPGs largely contributes to the *lsd1* RCD[9], we hypothesized that nuSIB1 would counteractively modulate the LSD1-GLK interaction to reinforce the expression of PhANGs. Considering its prompt turnover via UPS-mediated proteolysis[12], nuSIB1 may rapidly intervene the LSD1-GLK interaction, resulting in nuSIB1-GLK interaction and reinforced expression of PhANGs, thereby contributing to cell death[9]. Alternatively, SA per se may interfere with the LSD1-GLK interaction, for instance, through the alteration of the protein conformation of LSD1 or GLKs or both. In fact, a previous report showed a redox-sensitive reconfiguration of LSD1 and a concurrent change of its interactome[15,33]. Thus, we examined the effect of SA on the LSD1-GLK1 interaction in Arabidopsis leaf protoplasts isolated from WT and the *sib1* mutant. We noticed that SA significantly hindered the LSD1-GLK1 interaction in WT but not in the *sib1* mutant (Fig. 7a), indicating that nuSIB1 rather than SA per se intervenes the LSD1-GLK1 interaction. To further elucidate the antagonistic action of nuSIB1 towards LSD1-GLK1 interaction, the dose-dependent impact of nuSIB1 was examined. For this, LSD1-GFP and GLK1-Myc were transiently coexpressed in Arabidopsis leaf protoplasts, along with different amounts of free RFP or SIB1-RFP. It should be noted that increasing doses of RFP or SIB1-RFP decline the expression of LSD1-GFP and GLK1-Myc, probably due to the diminished transfection efficiency by the excess amounts of constructs (Fig. 7b). Nonetheless, the relative amount of GLK1-Myc protein co-immunoprecipitated with LSD1-GFP was quantified using ImageJ following immunoblot analysis (Fig. 7c). The results showed a SIB1 dose-dependent inhibition of the LSD1-GLK1 interaction.

It is possible that nuSIB1 also interacts with LSD1 and the then released GLKs may interact with nuSIB1, promoting the expression of PhANGs. However, while the interaction between LSD1-GFP and LSD1-RFP was apparent, no interaction between

LSD1-RFP and SIB1-RFP was observed (Supplementary Fig. 4). It is likely that SA-induced nuSIB1 counteractively interacts with GLKs, which consequently enhances the level of $^1O_2$ and thereby activates an EX1-mediated cell death response (Fig. 7d). The rapid turnover of nuSIB1 via UPS[12] may turn LSD1-GLK interaction, repressing the expression of PhANGs and GLK-mediated immune responses[6-8]. Such a dynamic regulatory circuit may be critical in sustaining photosynthetic and ROS homeostasis as well as SA-induced stress responses.

Discussion

LSD1 is present in both cytosol and nucleus. Cytosolic LSD1 is considered functioning as a scaffold protein holding its target proteins under non-stress conditions. According to earlier reports, LSD1-retained proteins include BASIC LEUCINE ZIPPER10 (bZIP10) and METACASPASE1 (MC1), which participate in inducing cell death in the Arabidopsis *lsd1* mutant and during plant-pathogen interaction[34,35]. Increased cellular stress levels seem to release the LSD1-retained proteins, facilitating cell death response. LSD1 also interacts with the plasma membrane protein GSH-induced LITAF domain protein (GILP), which serves as a negative regulator of cell death[36]. Neither a recent study[33] which intended to identify LSD1-associated proteins using the tandem affinity purification (TAP) assay nor our IP-MS assay identified the positive or negative regulators of cell death. The TAP assay and IP-MS analysis found only one common protein, UDP-glucose 6-dehydrogenase family protein[33] (Supplementary Table 1). We also identified catalase 3 (CAT3), a detoxifier of ROS, which interaction with LSD1 was identified via IP-MS analysis by another group[37] (Supplementary Table 1). CAT3 appears to antagonize *lsd1* RCD[37]. At present, we reasoned that such inconsistent identification of LSD1-associated proteins by several groups is likely related to the different source materials (e.g. cell culture versus plants), methods, and transient or weak interaction with LSD1. Nonetheless, previous studies on LSD1 and our findings support the increasing notion that LSD1 functions 1. as a scaffold protein in the cytosol to inhibit positive regulators of cell death (bZIP10 and MC1), 2. as a stimulator of the negative regulators of cell death (GILP and CAT3), and 3. as a transcription coregulator in the nucleus.

SIB1, a transcription coregulator, rapidly accumulates in both the nucleus and chloroplasts in response to an increase in foliar SA[9]. The nuSIB1 interacts with GLKs to stimulate their activity, resulting in the elevated expression of PhANGs, while the cpSIB1 downregulates the expression of PhAPGs. This SIB1-driven molecular episode, a so-called "genomes-uncoupled expression", directs a $^1O_2$ burst in the chloroplasts because of photoinhibition (resulted from the excess light energy and reduced photosynthetic capacity) and contributes to the *lsd1* RCD through the activation of EX1-mediated RS[9]. We now found that LSD1 also functions as a negative regulator of GLKs. The LSD1-GLK interaction in the nucleus (Figs 1 and 2) led to the repression of PhANGs, especially genes encoding LHCBs and chlorophyll biosynthesis enzymes (Fig. 5). By contrast, loss of LSD1 resulted in a higher expression of PhANGs and an increase in TBS in the Mg-branch as compared to WT plants (Fig. 6). The impact of loss- and gain-of-function of LSD1 towards the transcript abundances of GLK target genes suggest a steady-state LSD1-GLK interaction in WT plants grown under normal growth conditions (Figs. 5a-c and 6a,b). Given that the elevated expression of PhANGs directed by SIB1-GLK interaction stimulates *lsd1* RCD[9], it is rational to assume that the SA-induced nuSIB1 interferes with the LSD1-GLK interaction to ensure a SIB1-GLK-mediated expression of PhANGs. Indeed, the Co-IP/immunoblot assay confirmed the negative impact of nuSIB1 on the LSD1-GLK interaction (Fig. 7a-c). We inferred that such opposing regulation of GLKs by SIB1 and LSD1 might be vital to maintain $^1O_2$ homeostasis in chloroplasts during and after SA-increasing stress conditions (Fig. 7d).

Since both abiotic and biotic stressors promote *lsd1* RCD[13-17,20,38], it is conceivable that the repression of PhANGs by LSD1-GLK interaction would be an integral part of regulating $^1O_2$ and minimizing photodamage in chloroplasts under various stress conditions. This notion also raises a plausible idea that GUN1-mediated RS, which transcriptionally represses PhANGs, may further facilitate plant stress/acclimation responses. Consistently, loss of GUN1 compromises the plant resistance towards heat, water, drought, cold, and high-light stresses[39-43]. Moreover,

gun1 mutant plants exhibit an increased level of ROS under these stress conditions[39,41,43]. However, how the GUN1-mediated RS facilitates plant stress tolerance remained an enigma. Now, according to our present studies on SIB1 and LSD1, GLKs may probably play a key role in GUN1-RS-mediated stress responses. Besides, like SIB1, GLK1 also undergoes post-translational regulation through UPS[24]. It seems that various signaling components, such as GUN1, SIB1, and LSD1, and the posttranslational UPS target GLKs for photosynthesis and ROS homeostasis as well as SA-mediated stress responses.

Methods

Plant materials and growth conditions

The seeds used in this study were derived from *Arabidopsis thaliana* Columbia-0 (Col-0) ecotype and were harvested from plants grown under continuous light (CL; 100 $\mu mol \cdot m^{-2} \cdot s^{-1}$) at 22 ± 2 °C. Arabidopsis mutant seeds used in this study, including *lsd1-2* (SALK_042687)[9] and *glk1 glk2* (*Atglk1.1; Atglk2.1*)[5] were obtained from the Nottingham Arabidopsis Stock Centre (NASC). *flu5c* has been described previously[31]. The double and triple mutants in the *lsd1-2* background including *lsd1 flu* and *lsd1 glk1 glk2* were generated by crossing the homozygous plants. The genotypes of all mutants were confirmed by PCR-based analyses. Primer sequences used for PCR are listed in Supplementary Table 2.

Seeds were surface sterilized with 70% (v/v) ethanol containing 0.05% (v/v) Triton X-100 (Sigma-Aldrich) for 5 min and washed five times with sterile distilled water. The sterile seeds were plated on Murashige and Skoog (MS) medium (Duchefa Biochemie) with 0.7% (w/v) agar (Duchefa Biochemie) and stratified at 4 °C in darkness for two days prior to placing in a growth chamber (CU-41L4; Percival Scientific) with CL condition.

Generation of *LSD1* overexpression line

The stop-codon-less *LSD1* coding sequence (CDS) was cloned into the modified

pCAMBIA3300 binary vector containing the 35S promoter, a NcoI restriction site, and the *EGFP*. Arabidopsis stable transgenic lines were generated by a floral dip transformation procedure[45] with *Agrobacterium tumefaciens* strain GV3101. Homozygous transgenic lines were selected on MS medium containing 12.5 mg/l glufosinate-ammonium (Sigma-Aldrich).

RNA extraction and RT-quantitative PCR (RT-qPCR)

Total RNA was isolated from leaf tissues using the Spectrum Plant Total RNA Kit (Sigma-Aldrich) according to the manufacturer's instructions. The concentration of RNA was determined using the ultraviolet-visible spectrophotometer (NanoDrop™, Thermo Fisher Scientific), and the quality of RNA was evaluated by the measurement of the A260/A280 ratio. cDNA synthesis was performed with 1 μg of total RNA using the PrimeScript™ RT Reagent Kit (Takara) following the manufacturer's instructions. The RT-qPCR was performed on QuantStudio™ Flex Real-Time PCR System (Applied Biosystems) using iTaq Universal SYBR Green PCR master mix (Bio-Rad). The relative transcript level was calculated by the ddCt method[46] and normalized to the *ACTIN2* (AT3G18780) gene transcript level. The sequences of the primers used for RT-qPCR are listed in Supplementary Table 2.

Co-immunoprecipitation (Co-IP) assay

Co-IP assays were performed using *Nicotiana benthamiana* or Arabidopsis leaf protoplasts transiently coexpressed with the indicated combination of proteins. For the Co-IP assays in *N. benthamiana*, the *35S:LSD1-sGFP*, *35S:GLK1-4xMyc*, and *35S:GLK2-4xMyc* constructs were created as described previously[9]. Briefly, pDONR/Zeo entry vector (Thermo Scientific) containing the stop codon-less full-length CDS of *LSD1*, *GLK1*, or *GLK2* was recombined into the destination vector pGWB605 for C-terminal fusion with sGFP or pGWB617 for C-terminal fusion with 4xMyc through the Gateway LR reaction (Thermo Scientific). For the *35S:GLK1-4xMyc* and *35S:GLK2-4xMyc* constructs, a linker DNA encoding Gly-Gly-Ser-Gly-Gly-Ser was added between 4xMyc tag and GLK1 or GLK2 to

increase conformational flexibility of the fusion protein as described previously[24]. The same procedures were used to create the *35S:GLK1$_{\Delta CT}$-4xMyc* and *35S:GLK2$_{\Delta CT}$-4xMyc* constructs. The different combinations of selected vectors were coexpressed in 4-week-old *Nicotiana benthamiana* leaves by Agrobacterium-mediated leaf infiltration as described by *Boruc et al.*[47]. For the Co-IP assays in Arabidopsis leaf protoplasts, the *35S:LSD1-sGFP*, *35S:GLK1-4xMyc*, *35S:SIB1-RFP*, and *35S:LSD1-RFP* were cloned into the pSAT6 vector[48]. The isolation and transfection of Arabidopsis leaf protoplasts were performed as described previously[49]. The indicated combination of vectors was cotransfected into protoplasts (3×10^6) isolated from 4-week-old plants of WT or *sib1*.

Total protein was extracted using an IP buffer containing 50 mM Tris-HCl (pH 7.5), 150 mM NaCl, 0.5mM EDTA, 10% (v/v) glycerol, 1% (v/v) Nonidet P-40 (NP-40), 1% deoxycholate, 0.1% (w/v) SDS, 1× cOmplete protease inhibitor cocktail (Roche), 1 mM PMSF, and 50 μM MG132. The protein extracts were incubated with 20 μL of GFP-Trap magnetic agarose beads (GFP-TrapMA, Chromotek) for 2 h at 4 °C by vertical rotation (10 rpm). After incubation, the beads were washed five times with the washing buffer containing 10 mM Tris-HCl (pH 7.5), 150 mM NaCl, 0.5 mM EDTA, 1 mM PMSF, 50 μM MG132, and 1× cOmplete protease inhibitor cocktail. The immunoprecipitated proteins were then eluted with 2 × SDS protein sample buffer [120 mM Tris-HCl (pH 6.8), 20% (v/v) glycerol, 4% (v/w) SDS, 0.04% (v/w) bromophenol blue, and 10% (v/v) β-mercaptoethanol] for 10 min at 95 °C. The eluates were subjected to 10% SDS-PAGE gels, and the interaction between coexpressed proteins was examined by immunoblot analyses using a mouse anti-Myc monoclonal antibody (1:10,000; Cell Signaling Technology), a rat anti-RFP monoclonal antibody (1:10,000; Chromotek), and a mouse anti-GFP monoclonal antibody (1:5,000; Roche).

ChIP-qPCR assays

ChIP assays were performed using Arabidopsis leaf protoplasts as described

404 previously[9,49,50]. Briefly, 1mg of pSAT6 vectors containing *35S:GLK1-4xMyc* DNA
405 were transfected with or without pSAT6 vector containing *35S:LSD1-RFP* DNA into
406 Arabidopsis leaf protoplasts (2×10^7) isolated from 4-week-old *lsd1 glk1 glk2* triple
407 mutant plants grown under 10-h light/14-h dark conditions at a light intensity of 100
408 μmol $m^{-2}s^{-1}$. Afterward, the protoplasts were incubated at 24 °C for 16 h under dim
409 light conditions. The protoplast chromatins were crosslinked by 1% (v/v)
410 formaldehyde in 1 X PBS (pH 7.4) for 10 min and quenched with 0.1 M glycine for 5
411 min. After isolating nuclei from the protoplasts, the chromatins were sheared by
412 sonication into a major size of around 500 bp. The lysates were diluted with 10× ChIP
413 dilution buffer [1% (v/v) Triton X-100, 2 mM EDTA, 20 mM Tris–HCl (pH 8.0), 150
414 mM NaCl, 50 μM MG132, 1 mM PMSF, and 1× protease inhibitor cocktail] and
415 precleared by incubation with 50 μl Protein-A agarose beads/Salmon sperm DNA
416 (Millipore) at 4 °C for 1 h. The samples were then incubated with anti-Myc
417 monoclonal antibodies (1:10,000; Cell Signaling Technology) at 4 °C overnight. To
418 determine nonspecific binding of DNA on beads, ChIP assays were also performed
419 without antibody. After washing the beads[50], the immunocomplexes were eluted with
420 elution buffer containing 1% (w/v) SDS and 100 mM $NaHCO_3$. The eluates were
421 treated with proteinase K for 1 h at 37 °C after reverse cross-linking. The bound DNA
422 fragments were purified according to *Lee et al.*[50] and precipitated with ethanol in the
423 presence of glycogen. The purified DNA was dissolved in water. qPCRs were
424 performed on bound and input DNAs. The primers for each tested gene are listed in
425 Supplementary Table 2. The amount of DNA enriched by the anti-Myc antibody was
426 calculated in comparison with the respective input DNA used for each ChIP analysis.
427 Afterward, the enrichment was calculated by normalizing against the corresponding
428 control sample (without antibody).

429 **Production of recombinant proteins**

430 To produce recombinant proteins of LSD1, GLK1, GLK2, and the truncated GLK2
431 variants (247-386 and 296-386), the coding sequences (CDS) of genes were cloned
432 into the modified pET21b (Novagen) expression vector after adding a cleavage site

for the tobacco etch virus (TEV) protease to the 5' end of the CDSs. The recombinant proteins with a cleavable N-terminal 10xHis-MsyB tag were expressed in *E. coli* BL21 (DE3). After culturing the cells at 37 °C until OD_{600} 0.6, recombinant proteins were induced by the addition of 0.3 mM isopropyl-β-D-thiogalactopyranoside (IPTG) for 12 h at 16 °C. Cells were pelleted by centrifugation and resuspended with buffer A [(50 mM Tris (pH 8.0), 200 mM NaCl, and 1 mM PMSF]. The cells were lysed by high-pressure homogenizer at 600-800 bar and then centrifuged at 17,000 rpm for 50 min. Each soluble fraction was passed over a Ni-NTA column (Novagen) and eluted with buffer containing 25 mM Tris (pH 8.0), 200 mM NaCl, and 200 mM Imidazole. Subsequently, the eluates containing recombinant proteins with 10×His-MsyB tag were further purified by anion-exchange column (Source-15Q; GE Healthcare). The 10xHis-MSB tag was cleaved by TEV protease at 4 °C overnight and removed by anion-exchange column. Untagged recombinant proteins were then concentrated and further purified by size-exclusion chromatography (Superdex 200 Increase10/300 GL; GE Healthcare) in buffer containing 20 mM Tris (pH 8.0), 200 mM NaCl and 3 mM DTT. The peak fractions of each protein were pooled together and used for gel filtration assay.

Gel filtration assay

The recombinant proteins purified as described above were subjected to gel filtration assay (Superdex 200 Increase10/300 GL; GE Healthcare) in buffer containing 20 mM Tris (pH 8.0), 200 mM NaCl, and 3 mM DTT. A mixture of the purified LSD1 and GLK1 (or GLK2) proteins was incubated at 4 °C for 1 h before gel filtration assay. Samples from relevant fractions were applied to SDS-PAGE and visualized by Coomassie blue staining. Same procedures were used to examine the interaction of LSD1 with the truncated variants of GLK2 proteins.

Measuring ALA synthesis rate

The ALA synthesis rate was quantified as previously described[29]. The CL-grown 16-day-old plants of WT, *flu*, *lsd1*, and *lsd1 flu* were vacuum-infiltrated for 5 min with

an 80 mM levulinic acid (Sigma) solution containing 10mM KH_2PO_4 (pH 7.2) and 0.5% (v/v) Tween 20. After 1 hour incubation at room temperature under CL, samples were immediately frozen in liquid nitrogen and then homogenized in 4% (v/v) TCA. The homogenates were lysed at 95 °C for 15 min, cooled on ice for 2 min, and filtrated with 0.45 μm cellulose acetate membrane filters (Sterlitech). The filtrated lysates were neutralized with an equal volume of 0.5 M NaH_2PO_4 (pH 7.5). Afterward, ethylacetoacetate (1/5) was added and then the samples incubated at 95 °C for 10 min. After cooling on ice for 5 min, the extracts were mixed with the same volume of fresh Ehrlich's reagent [0.2 g *p*-dimethylaminobenzaldehyde (Sigma-Aldrich), 8.4ml acetic acid, and 1.6 ml 70% (v/v) perchloric acid (Sigma-Aldrich)] and centrifuged at 14,000 g for 5 min (at 4 °C). The OD of each supernatant was measured at 553 nm using the NanoDrop 2000 (Thermo Fisher Scientific). The amount of δ-ALA was calculated using a coefficient of 7.45×10^4 mol^{-1} cm^{-1}.

Gene ontology (GO) enrichment analysis

The individual RNA-seq data using the *lsd1* and *glk1 glk2*, analyzed in Fig. 5a, were previously published by *Lv et al.*[9] and *Ni et al.*[23], respectively. The GO enrichment analysis of the selected genes shown in Supplementary Data 4 was performed on gprofiler at https://biit.cs.ut.ee/gprofiler and represents the significantly enriched GO terms in the data set of biological processes (BP) with a significance of *P*-value < 0.05.

Pigment analysis

The levels of chlorophyll and Pchlide were measured in 10-day-old plants of WT, *flu*, *lsd1*, and *lsd1 flu* as described by *Lichtenthaler*[51] and *Goslings et al.*[29], respectively.

References

1 Nott, A., Jung, H. S., Koussevitzky, S. & Chory, J. Plastid-to-nucleus retrograde signaling. *Annu Rev Plant Biol* **57**, 739-759 (2006).

2 Chan, K. X., Phua, S. Y., Crisp, P., McQuinn, R. & Pogson, B. J. Learning the Languages of the Chloroplast: Retrograde Signaling and Beyond. *Annu Rev*

Plant Biol **67**, 25-53 (2016).

3 Waters, M. T. *et al.* GLK transcription factors coordinate expression of the photosynthetic apparatus in Arabidopsis. *Plant Cell* **21**, 1109-1128 (2009).

4 Martin, G. *et al.* Phytochrome and retrograde signalling pathways converge to antagonistically regulate a light-induced transcriptional network. *Nat Commun* **7**, 11431 (2016).

5 Fitter, D. W., Martin, D. J., Copley, M. J., Scotland, R. W. & Langdale, J. A. GLK gene pairs regulate chloroplast development in diverse plant species. *Plant J* **31**, 713-727 (2002).

6 Savitch, L. V., Subramaniam, R., Allard, G. C. & Singh, J. The GLK1 'regulon' encodes disease defense related proteins and confers resistance to Fusarium graminearum in Arabidopsis. *Biochem Biophys Res Commun* **359**, 234-238 (2007).

7 Murmu, J. *et al.* Arabidopsis GOLDEN2-LIKE (GLK) transcription factors activate jasmonic acid (JA)-dependent disease susceptibility to the biotrophic pathogen Hyaloperonospora arabidopsidis, as well as JA-independent plant immunity against the necrotrophic pathogen Botrytis cinerea. *Mol Plant Pathol* **15**, 174-184 (2014).

8 Han, X. Y. *et al.* GOLDEN2-LIKE transcription factors coordinate the tolerance to Cucumber mosaic virus in Arabidopsis. *Biochem Biophys Res Commun* **477**, 626-632 (2016).

9 Lv, R. *et al.* Uncoupled Expression of Nuclear and Plastid Photosynthesis-Associated Genes Contributes to Cell Death in a Lesion Mimic Mutant. *Plant Cell* **31**, 210-230 (2019).

10 Lai, Z. *et al.* Arabidopsis sigma factor binding proteins are activators of the WRKY33 transcription factor in plant defense. *Plant Cell* **23**, 3824-3841 (2011).

11 Dogra, V., Li, M., Singh, S., Li, M. & Kim, C. Oxidative post-translational modification of EXECUTER1 is required for singlet oxygen sensing in plastids. *Nat Commun* **10**, 2834 (2019).

12 Li, Z. *et al.* N-Terminal Acetylation Stabilizes SIGMA FACTOR BINDING PROTEIN1 Involved in Salicylic Acid-Primed Cell Death. *Plant Physiol* **183**, 358-370 (2020).

13 Muhlenbock, P. *et al.* Chloroplast signaling and LESION SIMULATING DISEASE1 regulate crosstalk between light acclimation and immunity in Arabidopsis. *Plant Cell* **20**, 2339-2356 (2008).

14 Jabs, T., Dietrich, R. A. & Dangl, J. L. Initiation of runaway cell death in an Arabidopsis mutant by extracellular superoxide. *Science* **273**, 1853-1856 (1996).

15 Dietrich, R. A., Richberg, M. H., Schmidt, R., Dean, C. & Dangl, J. L. A novel zinc finger protein is encoded by the Arabidopsis LSD1 gene and functions as a negative regulator of plant cell death. *Cell* **88**, 685-694 (1997).

16 Muhlenbock, P., Plaszczyca, M., Plaszczyca, M., Mellerowicz, E. & Karpinski, S. Lysigenous aerenchyma formation in Arabidopsis is controlled by LESION

SIMULATING DISEASE1. *Plant Cell* **19**, 3819-3830 (2007).

17 Huang, X., Li, Y., Zhang, X., Zuo, J. & Yang, S. The Arabidopsis LSD1 gene plays an important role in the regulation of low temperature-dependent cell death. *New Phytol* **187**, 301-312 (2010).

18 Karpinski, S., Szechynska-Hebda, M., Wituszynska, W. & Burdiak, P. Light acclimation, retrograde signalling, cell death and immune defences in plants. *Plant Cell Environ* **36**, 736-744 (2013).

19 Chai, T., Zhou, J., Liu, J. & Xing, D. LSD1 and HY5 antagonistically regulate red light induced-programmed cell death in Arabidopsis. *Front Plant Sci* **6**, 292 (2015).

20 Rusaczonek, A. *et al.* Role of phytochromes A and B in the regulation of cell death and acclimatory responses to UV stress in Arabidopsis thaliana. *J Exp Bot* **66**, 6679-6695 (2015).

21 Rossini, L., Cribb, L., Martin, D. J. & Langdale, J. A. The maize golden2 gene defines a novel class of transcriptional regulators in plants. *Plant Cell* **13**, 1231-1244 (2001).

22 Bravo-Garcia, A., Yasumura, Y. & Langdale, J. A. Specialization of the Golden2-like regulatory pathway during land plant evolution. *New Phytol* **183**, 133-141 (2009).

23 Ni, F. *et al.* Turnip Yellow Mosaic Virus P69 Interacts with and Suppresses GLK Transcription Factors to Cause Pale-Green Symptoms in Arabidopsis. *Mol Plant* **10**, 764-766 (2017).

24 Tokumaru, M. *et al.* Ubiquitin-Proteasome Dependent Regulation of the GOLDEN2-LIKE 1 Transcription Factor in Response to Plastid Signals. *Plant Physiol* **173**, 524-535 (2017).

25 Waters, M. T., Moylan, E. C. & Langdale, J. A. GLK transcription factors regulate chloroplast development in a cell-autonomous manner. *Plant J* **56**, 432-444 (2008).

26 Nandi, D. L. & Shemin, D. Delta-aminolevulinic acid dehydratase of Rhodopseudomonas spheroides. 3. Mechanism of porphobilinogen synthesis. *J Biol Chem* **243**, 1236-1242 (1968).

27 Beale, S. I. & Castelfranco, P. A. The Biosynthesis of delta-Aminolevulinic Acid in Higher Plants: I. Accumulation of delta-Aminolevulinic Acid in Greening Plant Tissues. *Plant Physiol* **53**, 291-296 (1974).

28 Hou, Z., Yang, Y., Hedtke, B. & Grimm, B. Fluorescence in blue light (FLU) is involved in inactivation and localization of glutamyl-tRNA reductase during light exposure. *Plant J* **97**, 517-529 (2019).

29 Goslings, D. *et al.* Concurrent interactions of heme and FLU with Glu tRNA reductase (HEMA1), the target of metabolic feedback inhibition of tetrapyrrole biosynthesis, in dark- and light-grown Arabidopsis plants. *Plant J* **40**, 957-967 (2004).

30 Forreiter, C. & Apel, K. Light-independent and light-dependent protochlorophyllide-reducing activities and two distinct NADPH-protochlorophyllide oxidoreductase polypeptides in mountain pine

(Pinus mugo). *Planta* **190**, 536-545 (1993).

31 Meskauskiene, R. *et al.* FLU: a negative regulator of chlorophyll biosynthesis in Arabidopsis thaliana. *Proc Natl Acad Sci U S A* **98**, 12826-12831 (2001).

32 Tanaka, R., Kobayashi, K. & Masuda, T. Tetrapyrrole Metabolism in Arabidopsis thaliana. *Arabidopsis Book* **9**, e0145 (2011).

33 Czarnocka, W. *et al.* The dual role of LESION SIMULATING DISEASE 1 as a condition-dependent scaffold protein and transcription regulator. *Plant Cell Environ* **40**, 2644-2662 (2017).

34 Kaminaka, H. *et al.* bZIP10-LSD1 antagonism modulates basal defense and cell death in Arabidopsis following infection. *EMBO J* **25**, 4400-4411 (2006).

35 Coll, N. S. *et al.* Arabidopsis type I metacaspases control cell death. *Science* **330**, 1393-1397 (2010).

36 He, S. *et al.* The LSD1-interacting protein GILP is a LITAF domain protein that negatively regulates hypersensitive cell death in Arabidopsis. *PLoS One* **6**, e18750 (2011).

37 Li, Y., Chen, L., Mu, J. & Zuo, J. LESION SIMULATING DISEASE1 interacts with catalases to regulate hypersensitive cell death in Arabidopsis. *Plant Physiol* **163**, 1059-1070 (2013).

38 Torres, M. A., Jones, J. D. & Dangl, J. L. Pathogen-induced, NADPH oxidase-derived reactive oxygen intermediates suppress spread of cell death in Arabidopsis thaliana. *Nat Genet* **37**, 1130-1134 (2005).

39 Cheng, J. *et al.* Plastid signals confer Arabidopsis tolerance to water stress. *Z Naturforsch C* **66**, 47-54 (2011).

40 Miller, G. *et al.* Double mutants deficient in cytosolic and thylakoid ascorbate peroxidase reveal a complex mode of interaction between reactive oxygen species, plant development, and response to abiotic stresses. *Plant Physiol* **144**, 1777-1785 (2007).

41 Tang, H. *et al.* Plastid signals induce ALTERNATIVE OXIDASE expression to enhance the cold stress tolerance in Arabidopsis thaliana. *Plant Growth Regul* **74**, 275-283 (2014).

42 Zhang, Z. W. *et al.* The roles of two transcription factors, ABI4 and CBFA, in ABA and plastid signalling and stress responses. *Plant Mol Biol* **83**, 445-458 (2013).

43 Zhang, Z. W. *et al.* Mg-protoporphyrin, haem and sugar signals double cellular total RNA against herbicide and high-light-derived oxidative stress. *Plant Cell Environ* **34**, 1031-1042 (2011).

44 Lee, K. P., Kim, C., Landgraf, F. & Apel, K. EXECUTER1- and EXECUTER2-dependent transfer of stress-related signals from the plastid to the nucleus of Arabidopsis thaliana. *Proc Natl Acad Sci U S A* **104**, 10270-10275 (2007).

45 Clough, S. J. & Bent, A. F. Floral dip: a simplified method for Agrobacterium-mediated transformation of Arabidopsis thaliana. *Plant J* **16**, 735-743 (1998).

46 Livak, K. J. & Schmittgen, T. D. Analysis of relative gene expression data

using real-time quantitative PCR and the 2(-Delta Delta C(T)) Method. *Methods* **25**, 402-408 (2001).

47 Boruc, J. *et al.* Functional modules in the Arabidopsis core cell cycle binary protein-protein interaction network. *Plant Cell* **22**, 1264-1280 (2010).

48 Tzfira, T. *et al.* pSAT vectors: a modular series of plasmids for autofluorescent protein tagging and expression of multiple genes in plants. *Plant Mol Biol* **57**, 503-516 (2005).

49 Yoo, S. D., Cho, Y. H. & Sheen, J. Arabidopsis mesophyll protoplasts: a versatile cell system for transient gene expression analysis. *Nat Protoc* **2**, 1565-1572 (2007).

50 Lee, J. H., Jin, S., Kim, S. Y., Kim, W. & Ahn, J. H. A fast, efficient chromatin immunoprecipitation method for studying protein-DNA binding in Arabidopsis mesophyll protoplasts. *Plant Methods* **13**, 42 (2017).

51 Lichtenthaler, H. K. Chlorophylls and Carotenoids - Pigments of Photosynthetic Biomembranes. *Method Enzymol* **148**, 350-382 (1987).

Acknowledgements

We thank the Core Facility of Proteomics in Shanghai Center for Plant Stress Biology (PSC) for carrying out mass spectrometry. This research was supported by the Strategic Priority Research Program from the Chinese Academy of Sciences (Grant No. XDB27040102), the 100-Talent Program of the Chinese Academy of Sciences, and the National Natural Science Foundation of China (NSFC) (Grant No. 31871397) to C.K..

Author contributions

M.L., K.P.L., T.L., V.D., W.X., and C.K. designed the experiments. M.L., K.P.L., T.L., V.D., J.D., and M.S.L. performed the experiments. M.L. K.P.L., T.L., V.D., W.X., and C.K. analyzed the data. M.L., K.P.L., and C.K. wrote the manuscript. All authors discussed the results and reviewed the manuscript.

Competing interests: The authors declare no competing interests.

Supplementary Information:

Supplementary Figures 1-4

Supplementary Tables 1 and 2

Supplementary Data 1-4

Figure legends

Figure 1. LSD1 interacts with GLK1 and GLK2 *in vivo*. a, Bimolecular fluorescence complementation (BiFC) assays. The GLK1 and GLK2 fused with C-terminal part of YFP (YFP^C) were individually coexpressed with the N-terminal part of the YFP (YFP^N) tagged with LSD1 in *N. benthamiana* leaves. The combinations of LSD1-YFP^N+LSD1-YFP^C and LSD1-YFP^N+YFP^C were used as a positive and negative control, respectively. DAPI was used to stain the nucleus. All images were taken under the same scale (scale bars: 25 μm). Chl: Chlorophyll. **b**, Co-immunoprecipitation (Co-IP) analyses using *N. benthamiana* leaves transiently coexpressing LSD1-GFP and GLK1-Myc (or GLK2-Myc).

Figure 2. LSD1 interacts with GLK1 and GLK2 *in vitro*. a,**b**, Left panels: Gel filtration profiles of LSD1, GLK1, and LSD1-GLK1 complex (**a**) and LSD1, GLK2, and LSD1-GLK2 complex (**b**). A_{280}(mAU), micro-ultraviolet absorbance at the wavelength of 280 nm. Right panels: Coomassie blue staining of the peak fractions following SDS-PAGE. Numbers on top of SDS-PAGE panels indicate elution volume (ml). M, molecular weight ladder (kDa).

Figure 3. The conserved C-terminal region of GLK2 is required to interact with LSD1 *in vitro*. a, Schematic diagram of the predicted domain structure of GLK1 and GLK2 along with truncated variants of the GLK2 protein ($GLK2_{247\text{-}386}$ and $GLK2_{296\text{-}386}$). The DBD and GCT-box represent the DNA-binding domain and the conserved C-terminal domain of GLK2, respectively. The light grey box (residues 247-265) between the DBD and GCT-box is a small conserved region in the GLK2 proteins. **b**, Gel filtration assays showing the *in vitro* interaction between LSD1 and the truncated variants of GLK2 expressed in *E. coli*. Left panel: Gel filtration profiles of LSD1, truncated variants of GLK2 and complex of LSD1 with the truncated variants of GLK2. This experiment was repeated twice with similar results. A_{280}(mAU), micro-ultraviolet absorbance at the wavelength of 280 nm. Right panel: Coomassie blue staining of the peak fractions following SDS-PAGE, the numbers on top of SDS-PAGE panels indicate elution volume (ml). M, molecular weight ladder (kDa).

Figure 4. The conserved C-terminal region of GLKs is necessary to interact with

LSD1 *in vivo*. a, Subcellular localizations of intact GLKs (GLK1-GFP and GLK2-GFP) and C-terminal-deleted (including the small conserved region shown in Fig. 3a) GLKs (GLK1$_{\Delta CT}$-GFP and GLK2$_{\Delta CT}$-GFP) fused with GFP upon transient expression in *N. benthamiana* leaves. Chl: chlorophyll. **b,** Bimolecular fluorescence complementation (BiFC) assays. The intact and C-terminal-deleted GLKs fused with the C-terminal part of YFP (YFP^C) were individually coexpressed with the N-terminal part YFP (YFP^N) of the YFP^N-tagged LSD1 in *N. benthamiana* leaves. The combination of LSD1-YFP^N+YFP^C was used as a negative control. DAPI was used to stain the nucleus. All images in **a**,**b** were taken under the same scale (scale bars: 10 μm). **c,** Co-IP analyses using *N. benthamiana* leaves transiently coexpressing LSD1-GFP with GLK1-Myc, GLK1$_{\Delta CT}$-Myc, GLK2-Myc, or GLK2$_{\Delta CT}$-Myc.

Figure 5. Loss of function of LSD1 leads to the upregulation GLK target genes. a, Venn diagram showing the numbers of uncommon and overlapped genes between upregulated genes (395) in 17-d-old *lsd1*[9] and downregulated genes (936) in *glk1 glk2*[23]. **b**, Gene Ontology (GO) enrichment analysis towards the biological process of the overlapped genes in **a**. The GO enrichment analysis was performed as described in Methods. **c**, The relative expression levels of GLK1 and GLK2 target genes (*LHCBs* and *LHCA1*) along with *LSD1* were examined in 17-d-old CL-grown plants of wild-type (WT), *glk1 glk2*, and transgenic WT plants overexpressing GFP-tagged LSD1 under the control of the 35S promoter (oxLSD1-GFP) using RT-qPCR. *ACT2* was used as an internal standard for the analyses. The value represents means ± standard deviation (SD) (n=3). Lowercase letters indicate statistically significant differences between mean values ($P < 0.05$, one-way ANOVA with posthoc Tukey's HSD test). **d,** ChIP–qPCR results showing the effect of LSD1 overexpression on GLK1 binding to the promoter regions of its target genes (*LHCB1.4*, *LHCB3*, and *LHCB6*). 4xMyc-fused GLK1 (GLK1-Myc) was transiently expressed with (+ LSD1) or without LSD1-RFP (– LSD1) in Arabidopsis leaf protoplasts isolated from *lsd1 glk1 glk2* triple mutant. The enrichment value was normalized to the input sample and represents means ± SD from two independent ChIP assays. Asterisks denote statistically significant differences by Student's *t*-test ($P < 0.01$) from the value of –LSD1.

Figure 6. *lsd1* mutation leads to the transcriptional upregulation of chlorophyll synthesis genes. a, A schematic representation of the chlorophyll synthesis pathway.

b, The expression levels of chlorophyll synthesis genes represented in **a** were obtained from our previous study[9], and the relative transcript levels of chlorophyll synthesis genes in 17-d-old CL-grown *lsd1* mutants compared to wild type (WT) are represented. Error bars indicate SD (n=3). Asterisks indicate statistically significant differences (*$P < 0.05$; **$P < 0.01$) in the *lsd1* mutant determined by Student's *t*-test relative to wild type. ND: non-detected. Red triangles in **a**,**b** indicate the genes that are significantly upregulated in the *lsd1* mutant compared to WT. **c**, The levels of the δ-ALA synthesis rate under CL. The rate of ALA synthesis was measured in 16-d-old plants of WT, *flu*, *lsd1*, and *lsd1 flu* grown under CL. **d**, Relative levels of protochlorophyllide (Pchlide) in 10-d-old plants of WT, *flu*, *lsd1*, and *lsd1 flu* grown under CL and then transferred to the dark for 8 hours. Values in **c**,**d** represent means ± SD (n=3). Lowercase letters indicate significant differences between the indicated genotypes ($P < 0.05$, one-way ANOVA with posthoc Tukey's HSD test).

Figure 7. SA-induced SIB1 interferes with LSD1-GLK interaction. a, The effect of the SA-induced SIB1 on the LSD1-GLK1 interaction. For Co-IP analyses, *35S:LSD1-GFP* and *35S:GLK1-Myc* were transiently coexpressed in Arabidopsis leaf protoplasts. The protoplasts were treated with either mock or 0.2 mM SA for 5 hours. **b**, The dose-dependent impact of SIB1 on the LSD1-GLK1 interaction. As indicated, *35S:LSD1-GFP* and *35S:GLK1-Myc* were coexpressed in Arabidopsis leaf protoplasts isolated from WT plants along with different amounts (10 μg, 20 μg, or 40 μg) of a plasmid containing either free *35S:RFP* or *35S:SIB1-RFP*. The subsequent Co-IP and immunoblot results are shown. Three independent experiments were conducted with similar results, and representative results are shown in **a**,**b**. **c**, The signal intensity of eluted GLK1-Myc (from triplicate immunoblots in **b**) versus its input signal was quantified using the ImageJ software. Data are means ± SD (n=3). Asterisks denote statistically significant differences by Student's *t*-test (*$P < 0.05$, **$P < 0.01$, NS: not significant). **d**, Proposed model elucidates that SA-induced SIB1 antagonistically regulates LSD1-GLK interactions to reinforce the expression of PhANGs such as LHCBs and chlorophyll synthesis enzymes. The heightened expression of PhANGs eventually results in the enhanced generation of $^1O_2$, activating EX1-mediated RS (contributing to cell death)[9]. On the other hand, the UPS primes the SIB1 proteolysis[12], which would in turn facilitate LSD1-GLK interaction to avoid an excess expression of PhANGs and $^1O_2$ accumulation. The counteractive regulation of the GLKs by SIB1

and LSD1 seems to be vital to maintain $^1O_2$ homeostasis in chloroplasts during and after SA-increasing stress conditions.

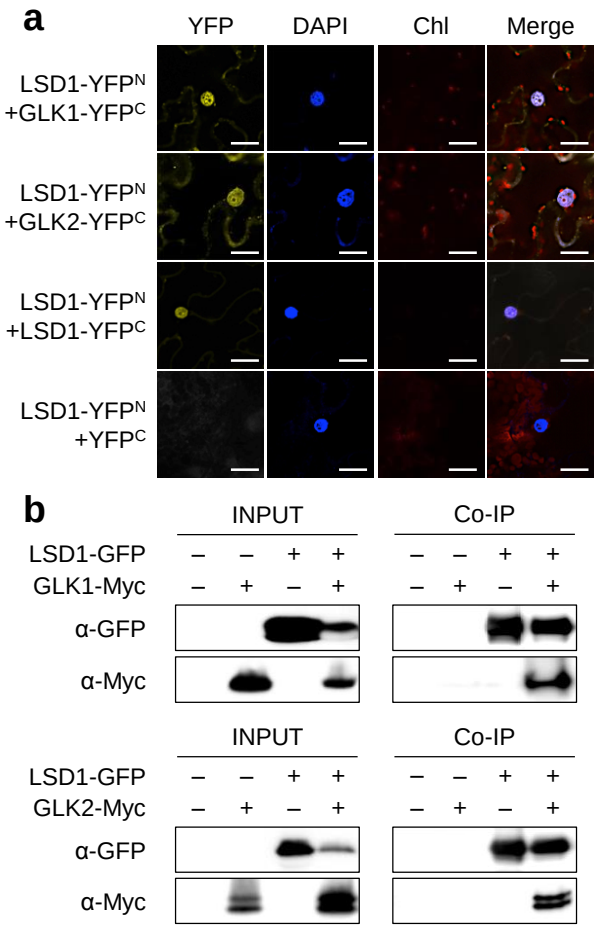

Figure 1. LSD1 interacts with GLK1 and GLK2 *in vivo*. a, Bimolecular fluorescence complementation (BiFC) assays. The GLK1 and GLK2 fused with C-terminal part of YFP (YFP^C) were individually coexpressed with the N-terminal part of the YFP (YFP^N) tagged with LSD1 in *N. benthamiana* leaves. The combinations of LSD1-YFP^N+LSD1-YFP^C and LSD1-YFP^N+YFP^C were used as a positive and negative control, respectively. DAPI was used to stain the nucleus. All images were taken under the same scale (scale bars: 25 µm). Chl: Chlorophyll. **b**, Co-immunoprecipitation (Co-IP) analyses using *N. benthamiana* leaves transiently coexpressing LSD1-GFP and GLK1-Myc (or GLK2-Myc).

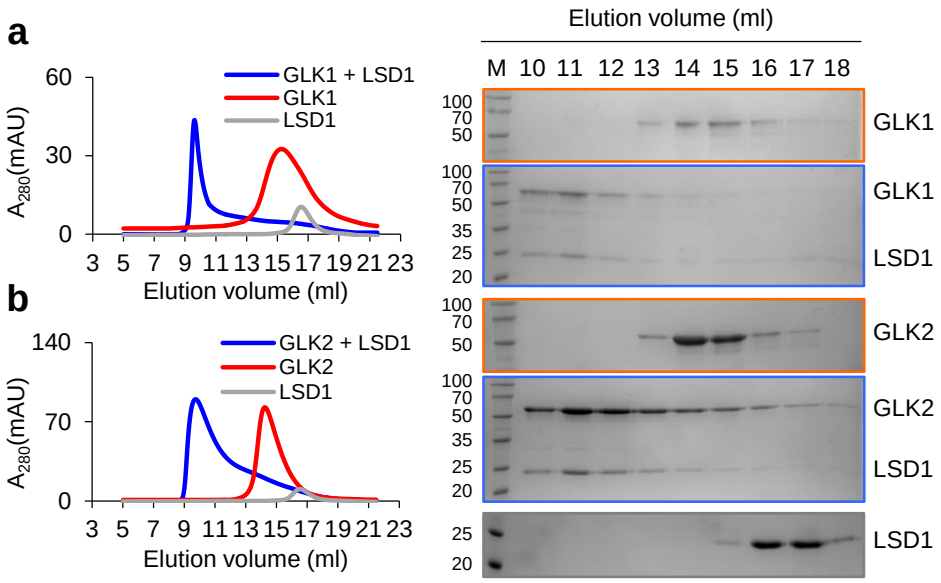

Figure 2. LSD1 interacts with GLK1 and GLK2 *in vitro*. a,**b**, Left panels: Gel filtration profiles of LSD1, GLK1, and LSD1-GLK1 complex (**a**) and LSD1, GLK2, and LSD1-GLK2 complex (**b**). A_{280}(mAU), micro-ultraviolet absorbance at the wavelength of 280 nm. Right panels: Coomassie blue staining of the peak fractions following SDS-PAGE. Numbers on top of SDS-PAGE panels indicate elution volume (ml). M, molecular weight ladder (kDa).

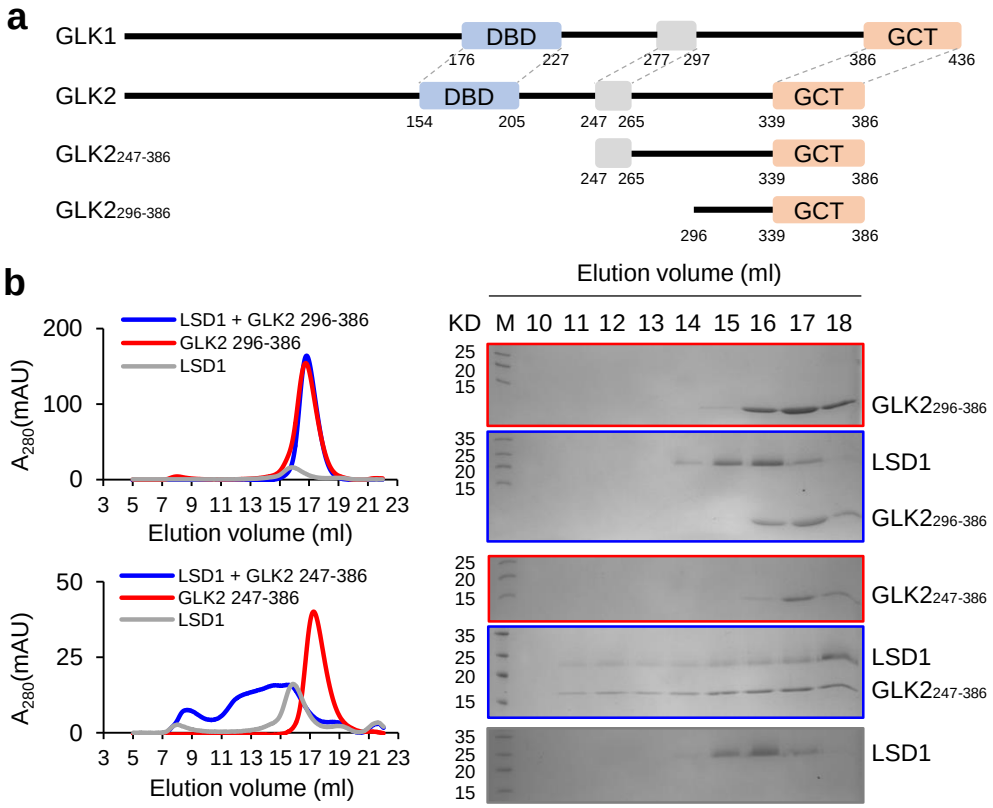

Figure 3. The conserved C-terminal region of GLK2 is required to interact with LSD1 *in vitro*. a, Schematic diagram of the predicted domain structure of GLK1 and GLK2 along with truncated variants of the GLK2 protein (GLK2247-386 and GLK2296-386). The DBD and GCT-box represent the DNA-binding domain and the conserved C-terminal domain of GLK2, respectively. The light grey box (residues 247-265) between the DBD and GCT-box is a small conserved region in the GLK2 proteins. **b**, Gel filtration assays showing the *in vitro* interaction between LSD1 and the truncated variants of GLK2 expressed in *E. coli*. Left panel: Gel filtration profiles of LSD1, truncated variants of GLK2 and complex of LSD1 with the truncated variants of GLK2. This experiment was repeated twice with similar results. A_{280}(mAU), micro-ultraviolet absorbance at the wavelength of 280 nm. Right panel: Coomassie blue staining of the peak fractions following SDS-PAGE, the numbers on top of SDS-PAGE panels indicate elution volume (ml). M, molecular weight ladder (kDa).

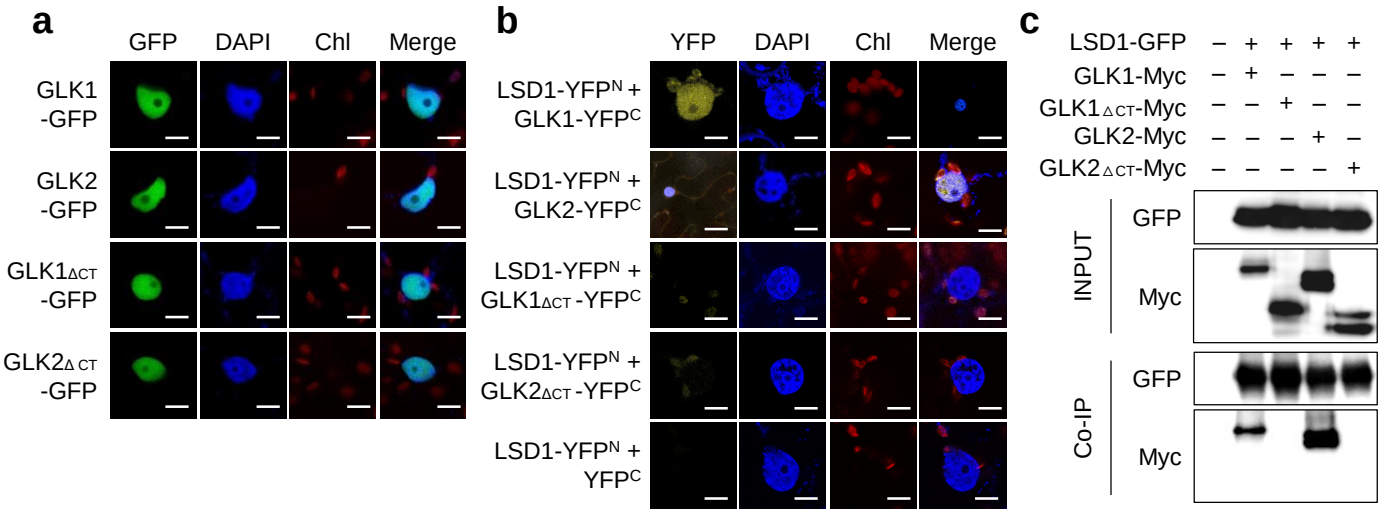

Figure 4. The conserved C-terminal region of GLKs is necessary to interact with LSD1 *in vivo*. a, Subcellular localizations of intact GLKs (GLK1-GFP and GLK2-GFP) and C-terminal-deleted (including the small conserved region shown in Fig. 3a) GLKs (GLK1$_{\Delta CT}$-GFP and GLK2$_{\Delta CT}$-GFP) fused with GFP upon transient expression in *N. benthamiana* leaves. Chl: chlorophyll. **b,** Bimolecular fluorescence complementation (BiFC) assays. The intact and C-terminal-deleted GLKs fused with the C-terminal part of YFP (YFP^C) were individually coexpressed with the N-terminal part YFP (YFP^N) of the YFP^N-tagged LSD1 in *N. benthamiana* leaves. The combination of LSD1-YFP^N+YFP^C was used as a negative control. DAPI was used to stain the nucleus. All images in **a**,**b** were taken under the same scale (scale bars: 10 μm). **c,** Co-IP analyses using *N. benthamiana* leaves transiently coexpressing LSD1-GFP with GLK1-Myc, GLK1$_{\Delta CT}$-Myc, GLK2-Myc, or GLK2$_{\Delta CT}$-Myc.

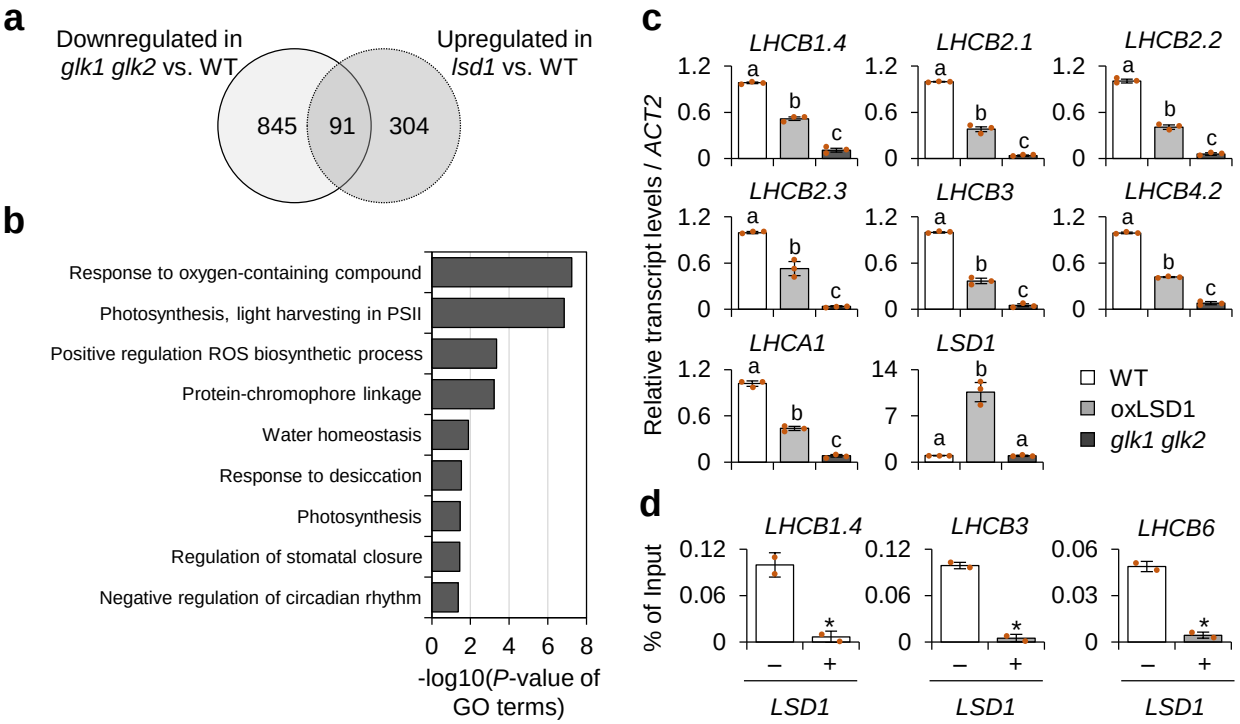

Figure 5. Loss of function of LSD1 leads to the upregulation GLK target genes. a, Venn diagram showing the numbers of uncommon and overlapped genes between upregulated genes (395) in 17-d-old *lsd1*[9] and downregulated genes (936) in *glk1 glk2*[23]. **b**, Gene Ontology (GO) enrichment analysis towards the biological process of the overlapped genes in **a**. The GO enrichment analysis was performed as described in Methods. **c**, The relative expression levels of GLK1 and GLK2 target genes (*LHCBs* and *LHCA1*) along with *LSD1* were examined in 17-d-old CL-grown plants of wild-type (WT), *glk1 glk2*, and transgenic WT plants overexpressing GFP-tagged LSD1 under the control of the 35S promoter (oxLSD1-GFP) using RT-qPCR. *ACT2* was used as an internal standard for the analyses. The value represents means ± standard deviation (SD) (n=3). Lowercase letters indicate statistically significant differences between mean values (P < 0.05, one-way ANOVA with posthoc Tukey's HSD test). **d,** ChIP–qPCR results showing the effect of LSD1 overexpression on GLK1 binding to the promoter regions of its target genes (*LHCB1.4*, *LHCB3,* and *LHCB6*). 4xMyc-fused GLK1 (GLK1-Myc) was transiently expressed with (+ LSD1) or without LSD1-RFP (– LSD1) in Arabidopsis leaf protoplasts isolated from *lsd1 glk1 glk2* triple mutant. The enrichment value was normalized to the input sample and represents means ± SD from two independent ChIP assays. Asterisks denote statistically significant differences by Student's *t*-test (*P* < 0.01) from the value of – LSD1.

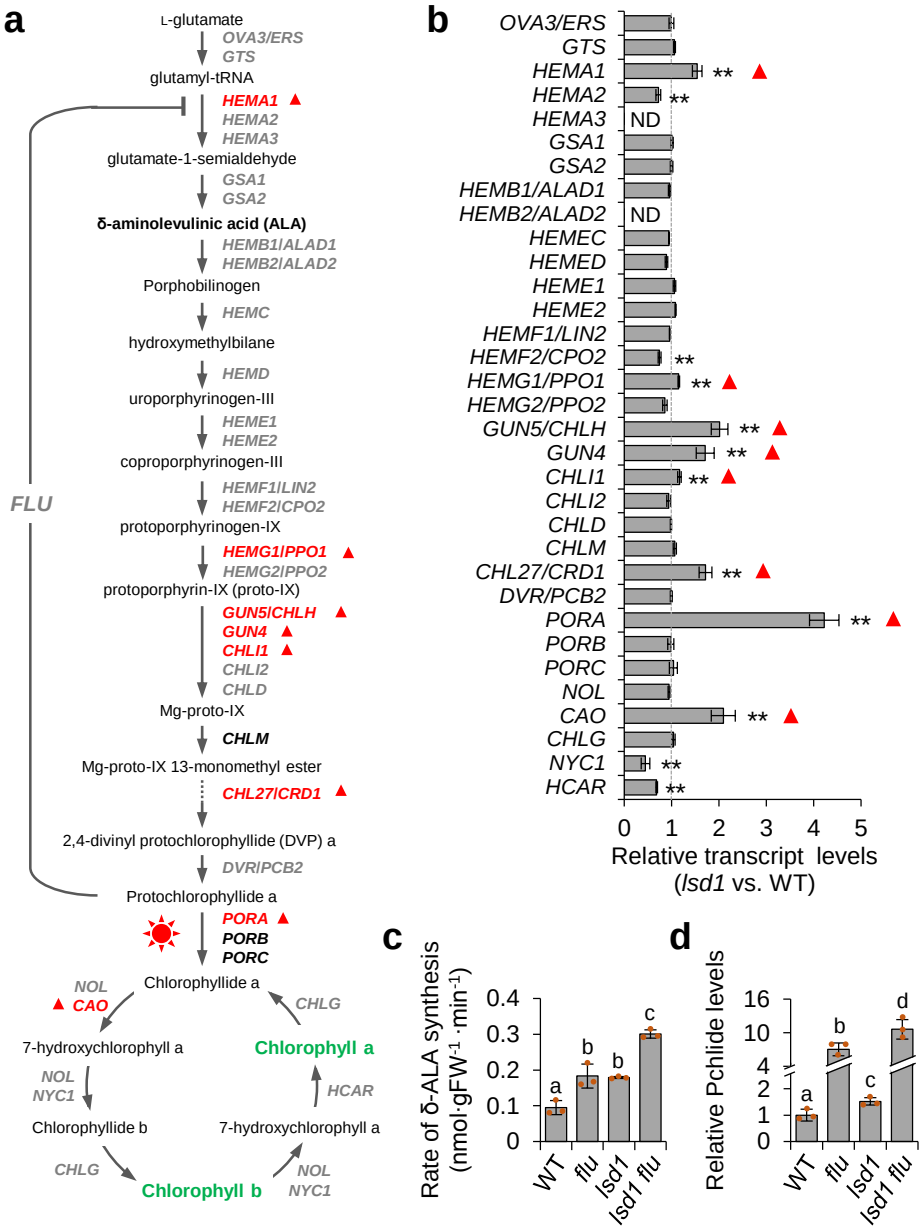

Figure 6. *lsd1* mutation leads to the transcriptional upregulation of chlorophyll synthesis genes. a, A schematic representation of the chlorophyll synthesis pathway. **b**, The expression levels of chlorophyll synthesis genes represented in **a** were obtained from our previous study[9], and the relative transcript levels of chlorophyll synthesis genes in 17-d-old CL-grown *lsd1* mutants compared to wild type (WT) are represented. Error bars indicate SD (n=3). Asterisks indicate statistically significant differences (**P* < 0.05; ***P* < 0.01) in the *lsd1* mutant determined by Student's *t*-test relative to wild type. ND: non-detected. Red triangles in **a**,**b** indicate the genes that are significantly upregulated in the *lsd1* mutant compared to WT. **c**, The levels of the δ-ALA synthesis rate under CL. The rate of ALA synthesis was measured in 16-d-old plants of WT, *flu*, *lsd1*, and *lsd1 flu* grown under CL. **d**, Relative levels of protochlorophyllide (Pchlide) in 10-d-old plants of WT, *flu*, *lsd1*, and *lsd1 flu* grown under CL and then transferred to the dark for 8 hours. Values in **c**,**d** represent means ± SD (n=3). Lowercase letters indicate significant differences between the indicated genotypes (*P* < 0.05, one-way ANOVA with posthoc Tukey's HSD test).

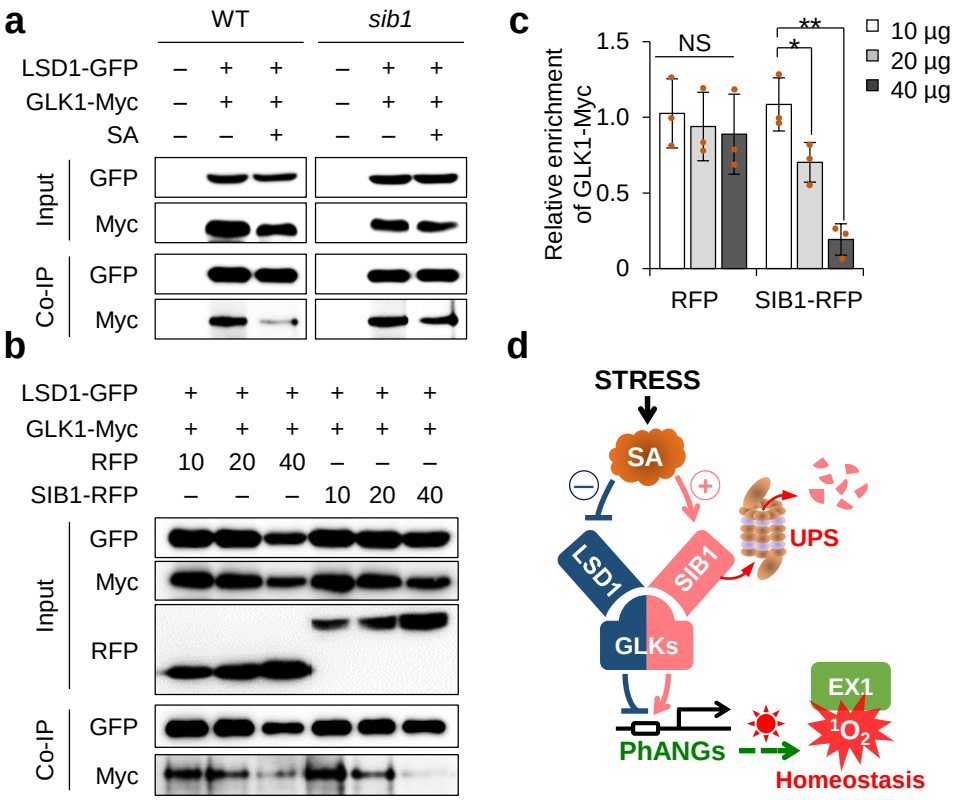

Figure 7. SA-induced SIB1 interferes with LSD1-GLK interaction. a, The effect of the SA-induced SIB1 on the LSD1-GLK1 interaction. For Co-IP analyses, *35S:LSD1-GFP* and *35S:GLK1-Myc* were transiently coexpressed in Arabidopsis leaf protoplasts. The protoplasts were treated with either mock or 0.2 mM SA for 5 hours. **b**, The dose-dependent impact of SIB1 on the LSD1-GLK1 interaction. As indicated, *35S:LSD1-GFP* and *35S:GLK1-Myc* were coexpressed in Arabidopsis leaf protoplasts isolated from WT plants along with different amounts (10 μg, 20 μg, or 40 μg) of a plasmid containing either free *35S:RFP* or *35S:SIB1-RFP*. The subsequent Co-IP and immunoblot results are shown. Three independent experiments were conducted with similar results, and representative results are shown in **a**,**b**. **c**, The signal intensity of eluted GLK1-Myc (from triplicate immunoblots in **b**) versus its input signal was quantified using the ImageJ software. Data are means ± SD (n=3). Asterisks denote statistically significant differences by Student's *t*-test (**P* < 0.05, ***P* < 0.01, NS: not significant). **d**, Proposed model elucidates that SA-induced SIB1 antagonistically regulates LSD1-GLK interactions to reinforce the expression of PhANGs such as LHCBs and chlorophyll synthesis enzymes. The heightened expression of PhANGs eventually results in the enhanced generation of $^1O_2$, activating EX1-mediated RS (contributing to cell death)[9]. On the other hand, the UPS primes the SIB1 proteolysis[12], which would in turn facilitate LSD1-GLK interaction to avoid an excess expression of PhANGs and $^1O_2$ accumulation. The counteractive regulation of the GLKs by SIB1 and LSD1 seems to be vital to maintain $^1O_2$ homeostasis in chloroplasts during and after SA-increasing stress conditions.